Saudi Pharmaceutical Journal 29 (2021) 1405–1415

Contents lists available at ScienceDirect

Saudi Pharmaceutical Journal

journal homepage: www.sciencedirect.com

Original article

Icariin regulates miR-23a-3p-mediated osteogenic differentiation of BMSCs via BMP-2/Smad5/Runx2 and WNT/β-catenin pathways in osteonecrosis of the femoral head

Xiao-yun Zhang [a,b,*], Hua-nan Li [a,c,*], Feng Chen [b], Yue-ping Chen [b], Yuan Chai [b], Jian-zhao Liao [b], Bin Gan [a], Ding-peng Chen [a], Song Li [a], Yong-qian Liu [a]

[a] Jiangxi University of Traditional Chinese Medicine, Nanchang 330004, China
[b] Department of Orthopedics, Ruikang Hospital Affiliated with Guangxi University of Chinese Medicine, Nanning 530011, China
[c] Department of Orthopedics, Hospital Affiliated with Jiangxi University of Traditional Chinese Medicine, Nanchang 330004, China

ARTICLE INFO

Article history:
Received 12 April 2021
Accepted 22 October 2021
Available online 29 October 2021

Keywords:
Icariin
miR-23a-3p
Osteonecrosis of the femoral head
BMP-2/Smad5/Runx2 pathway
WNT/β-catenin pathway

ABSTRACT

Icariin is commonly used for the clinical treatment of osteonecrosis of the femoral head (ONFH). miR-23a-3p plays a vital role in regulating the osteogenic differentiation of bone marrow-derived mesenchymal stem cells (BMSCs). The present study aimed to investigate the roles of icariin and miR-23a-3p in the osteogenic differentiation of BMSCs and an ONFH model. BMSCs were isolated and cultured in vitro using icariin-containing serum at various concentrations, and BMSCs were also transfected with a miR-23a inhibitor. The alkaline phosphatase (ALP) activity and cell viability as well as BMP-2/Smad5/Runx2 and WNT/β-catenin pathway-related mRNA and protein expression were measured in BMSCs. Additionally, a dual-luciferase reporter assay and pathway inhibitors were used to verify the relationship of icariin treatment/miR-23a and the above pathways. An ONFH rat model was established in vivo, and a 28-day gavage treatment and lentivirus transfection of miR-23a-3p inhibitor were performed. Then, bone biochemical markers (ELISA kits) in serum, femoral head (HE staining and Digital Radiography, DR) and the above pathway-related proteins were detected. Our results revealed that icariin treatment/miR-23a knockdown promoted BMSC viability and osteogenic differentiation as well as increased the mRNA and protein expression of BMP-2, BMP-4, Runx2, p-Smad5, Wnt1 and β-catenin in BMSCs and ONFH model rats. In addition, icariin treatment/miR-23a knockdown increased bone biochemical markers (ACP-5, BAP, NTXI, CTXI and OC) and improved ONFH in ONFH model rats. In addition, a dual-luciferase reporter assay verified that Runx2 was a direct target of miR-23a-3p. These data indicated that icariin promotes BMSC viability and osteogenic differentiation as well as improves ONFH by decreasing miR-23a-3p levels and regulating the BMP-2/Smad5/Runx2 and WNT/β-catenin pathways.

Abbreviations: BMSCs, bone marrow-derived mesenchymal stem cells; ONFH, osteonecrosis of the femoral head; BMP-2, bone morphogenetic protein-2; BMP-4, bone morphogenetic protein-4; DMEM, Dulbecco's modified Eagle's medium; FBS, fetal bovine serum; DR, Digital Radiography; OC, osteocalcin; BAP, bone-specific alkaline phosphatase; NTX-1, N-terminal telopeptides of type I collagen; CTX-1, C-terminal telopeptides of type I collagen; TRACP-5b, tartrate-resistant acid phosphatase 5b; RT-PCR, Real time PCR; SI, icariin-containing serum; LPS, lipopolysaccharide; HE, Hematoxylin-eosin.

* Corresponding authors at: Jiangxi University of Traditional Chinese Medicine, No. 1688 Meiling Avenue, Nanchang 330004, China (X. Zhang). Department of Orthopedics, Hospital Affiliated with Jiangxi University of Traditional Chinese Medicine, No. 445 Meiling Avenue, Nanchang 330004, China (H. Li).
E-mail addresses: zhangxiaoyun520@126.com (X.-y. Zhang), 20086170@jxutcm.edu.cn (H.-n. Li).

Peer review under responsibility of King Saud University.

Production and hosting by Elsevier

https://doi.org/10.1016/j.jsps.2021.10.009

1. Introduction

Osteonecrosis of the femoral head (ONFH), a progressive disease, causes the collapse of the joint cartilage and femoral head, which is accompanied with pain and gait disturbance (Karasuyama et al., 2015). Currently, over 30 million people suffer from ONFH globally, including more than 8 million individuals in China (Fang et al., 2019a; Wang et al., 2017). Delaying or reversing the progression of ONFH is a problem in clinical treatment. Clinically, Western medicine mainly adopts conservative treatment, which does not delay or reverse the progression of ONFH. Traditional Chinese medicine has been clinically verified in the treatment of ONFH and has attracted the attention of Western medicine. The Chinese herbal Huo-Gu formula (HGF) prevents femoral head collapse, delays total hip arthroplasty and maintains physical function in the treatment of ONFH (Huang et al., 2020). Qing'e pill and Salvia regulate bone formation and remodeling by suppressing osteoclasts (Shuai et al., 2014).

Epimedium brevicornu Maxim is a traditional Chinese medicine that has been used to attenuate inflammation and restore osteogenesis (Fang et al., 2019a; Wang et al., 2009). Icariin, a flavonoid isolated from *Epimedium brevicornu Maxim*, is the major effective active component. For thousands of years, icariin has been widely used in China, Japan and Korea as an aphrodisiac, tonic and anti-osteoporosis agent, as recorded in the Chinese Pharmacopeia. Previous studies have demonstrated that icariin is an effective treatment for bone metabolic-related diseases (Wang et al., 2018; Yu et al., 2019; Cheng et al., 2014). Icariin also stimulates the osteoblastic differentiation of BMSCs or long bone-derived cells, enhances bone healing, prevents osteoporosis and improves ONFH (Wang et al., 2018; Yu et al., 2019). Oral icariin treatment promotes bone formation by inhibiting bone resorption and improving peak bone mineral density and bone quality, which has significant importance for the prevention of osteoporosis and osteoporotic fractures caused by different reasons (Cheng et al., 2014).

Recent studies have emphasized the importance and significance of miRNAs in the pathogenesis, prevention and treatment of ONFH (Liao et al., 2019; Yuan et al., 2015). It has been reported that various miRNAs participate in the development of ONFH by regulating bone development and regeneration (Liao et al., 2019). Studies have demonstrated that miR-23a-3p is the most significantly upregulated miRNA in patients with ONFH, and it is significantly downregulated during osteogenic differentiation (Dong et al., 2017). Overexpression of miR-23a-3p inhibits osteogenic differentiation of BMSCs, whereas downregulation of miR-23a-3p enhances this process (Dai et al., 2019). In a preliminary experiment, we found that the expression of miR-23a-3p was significantly increased in ONFH rats, while icariin reduced the expression of miR-23a-3p (Supplemental Fig. 1A). However, no relevant research has been reported on the protective mechanism of icariin against ONFH or its relationship with miR-23a-3p.

The BMP 2/Smad5/Runx2 and WNT1/β-catenin pathways are the most important pathways in osteoblast proliferation and differentiation (Gu et al., 2018; Dai et al., 2013). Based on the above information, we infer that the therapeutic effects of icariin on ONFH are related to the miR-23a-3p, BMP 2/Smad5/Runx2 and WNT1/β-catenin pathways. Therefore, we isolated rat BMSCs and established a rat model of ONFH, and we then intragastrically administered icariin or co-cultured the cells followed by transfection of a miR-23a-3p inhibitor to elucidate the therapeutic mechanisms of icariin in ONFH and the roles of miR-23a-3p in osteogenic differentiation. The present study elucidated the therapeutic mechanism of icariin against ONFH and provided a scientific basis for the clinical application of icariin.

2. Materials and methods

2.1. Materials and reagents

Wistar rats were obtained from Laboratory Animal Management Center of Southern Medical University (SCXK(YUE)2016-0041). Dulbecco's modified Eagle's medium (DMEM) and fetal bovine serum (FBS) were purchased from Gibco (Grand Island, NY, USA). Anti-CD29, anti-CD34, anti-CD44 and anti-CD45 antibodies were purchased from Abcam (USA). Prime Script RT Master Mix was purchased from Takara (DaLian, China). ITaq Universal SYBR Green Supermix was purchased from Bio-Rad (Hercules, CA, USA). Lentivirus LV3-pGLV-h1-GFP-puro-miR-23a-3p inhibitor or LV3-pGLV-h1-GFP-puro-NC was purchased from Youdi Biotechnology (Guangzhou, China). Icarin (HPLC > 94%) was purchased from Sigma-Aldrich (Shanghai, #I1286, China), and its chemical characterization is provided in Supplemental Fig. 2. Icarin was prepared into a 50 mg/mL suspension with normal saline for intragastric administration.

2.2. Isolation, culture and identification of BMSCs

Primary rat BMSCs were harvested by flushing the bone marrow cavity of the femurs and tibias of 4-week-old rats. After anesthesia and execution, the femurs and tibias were removed, and the bone marrow contents were flushed out. The bone marrow contents were layered over the same volume of Ficoll-Paque (Absin, China) and centrifuged at 900*g* for 20 min at 4 °C. Next, the middle phase containing the mononuclear cell layer was removed and washed 2 times with washing buffer. Bone marrow mononuclear cells were cultured in osteogenic differentiation medium (Cyagen Biosciences, RAWMX-90021, USA) supplemented with 10% FBS, 100 U/mL penicillin and 100 U/mL streptomycin at 37 °C in a 5% CO_2 atmosphere (Thermo, USA). After 48 h, the nonadherent cells were removed, and the adherent cells were cultured in another flask (Yang et al., 2020; Farahzadi et al., 2020). The positive ratios of CD29, CD44, CD34 and CD45 antibodies were detected by flow cytometry (BD, Accuri C6, USA) to identify BMSCs.

2.3. Preparation of icariin-containing serum and its optimal concentration

To prepare icariin-containing serum (SI), 6-week-old Wistar rats were orally gavaged with 200 mg/kg icariin once a day for 7 days. After 7 days, rats were euthanized, and blood samples were collected. The serum was filtered and sterilized with 0.22 μm filter to obtain 15 mL of SI (Zhang et al., 2020).

BMSCs were seeded in 6-well plates and cultured in osteogenic induction medium supplemented with different concentrations of SI (2.5%, 5% and 10%) or cultured in icariin-free serum at the same ratio. After induction for 9 days, ALP activity was measured using an alkaline phosphatase kit (Nanjing Jiancheng, A059-2). The serum concentration corresponding to the highest ALP activity was the optimal concentration of SI, and it was used in subsequent experiments.

HPLC identification of the icariin in osteogenic induction medium supplemented with 10% SI or 10% icariin-free serum: Acetonitrile was added to the above medium to precipitate the proteins and the supernatant was evaporated to dryness. The residues were re-dissolved in acetonitrile and 20 μL aliquot was injected onto the HPLC column (Yin et al., 2014). The analytes were measured with a DionexU-3000 HPLC system with a xbridge amide column(150 m m × 4.6 mm). The mobile phase consisted of 100% acetonitrile (A) and 0.005% phosphoric acid in water (B), and was programmed

as follows: 0–30 min, 15–30% B; 30–60 min, 80% B. The flow rate was 2.0 mL/min and the ambient temperature was set at room temperature. UV detection was at a wavelength of 270 nm. HPLC results were shown in Supplemental Fig. 3.

2.4. Transfection of miR-23a-3p in BMSCs and grouping

The miR-23a-3p inhibitor (5′-GGAAAUCCCUGGCAAUGUGAU-3′) and negative control (5′-CUUAGGCAUUGCCAGCUCAAU-3′) were transfected into the lentiviral green fluorescent protein (GFP)-tagged vector, LV3-pGLV-h1-GFP-puro. Synthetic miRNA (1×10^9 transducing units/mL) was transfected into BMSCs according to the manufacturer's protocol. The most effective multiplicity of infection (MOI) was determined according to the pilot experiment. BMSCs were plated into 10 cm dishes at a density of 1×10^6 cells/dish in 5 mL of media and transduced using a GFP-tagged lentiviral vector (lenti-23a-inhibitor-GFP and lenti-GFP) at a MOI of 100 plaque-forming units/cell in the presence of 5 μL of polybrene (Merck KGaA). After lentiviral transduction, cells were selected with G418, and the stably transfected cell lines were then processed by monoclonal screening (Li et al., 2020). The transduced BMSCs were named miR-23a-3p-inhibitor BMSCs and miR-23a-3p-negative BMSC.

BMSCs were classified into the following 4 groups: the miR-23a-NC group (transfected with the miR-23a-3p negative control sequence), the miR-23a-NC + 10% SI group (transfected with the miR-23a-3p negative control sequence and cultured with 10% icariin-containing serum), the miR-23a inhibitor group (transfected with the miR-23a-3p inhibitor), and the miR-23a inhibitor + 10% SI group (transfected with the miR-23a-3p inhibitor and cultured with 10% icariin-containing serum).

2.5. Alizarin red staining

BMSCs were plated into 6-well plates at a density of 3×10^5 cells per well and cultured with differentiation medium. After 21 days of induction, cells were washed with PBS and then fixed with 95% ethanol for 30 min at room temperature. Cells were stained with 40 mmol/L alizarin red S solution (pH = 4.2) for 20 min at room temperature with gentle shaking (Farahzadi et al., 2016). After removal of the staining solution, cells were washed 5 times with distilled water. Finally, images were acquired with an Olympus fluorescence microscope (Olympus, CX71, Japan).

2.6. Cell viability assay

The above 4 groups of BMSCs were plated into 96-well plates (5×10^3 cells/well) in triplicate and cultured for 0, 72, 96 and 120 h. After culture, the CCK-8 working solution (Beyotime, C0037, China) was added to the wells for 1 h of incubation, and then cell viability was assessed daily by absorbance at 490 nm using a microplate reader (Model 680 Microplate Reader, Bio-Rad) (Cao et al., 2020).

2.7. Dual-luciferase reporter assay

To construct the Runx2 3′UTR plasmid, the full-length 3′UTR of Runx2 mRNA containing the putative miR-23a-3p-binding sequence was cloned into the pGL3 promotor vector (Promega, Madison, WI, USA). The putative miR-23a-3p recognition sites in the Runx2 3′UTR were mutated by site-directed mutagenesis. For the dual luciferase assay, BMSCs were transfected with 150 nM premiR-23a-3p or a negative precursor control using Lipofectamine 2000 (Invitrogen). After 24 h, cells were cotransfected with 200 ng of pRL-Runx2 and 100 ng of pGL3-luc as the internal control (G. Zhang et al., 2017). Cell extracts were prepared 48 h later, and the dual luciferase reporter assay (Promega) was performed according to the manufacturer's protocol.

2.8. RNA extraction and RT-qPCR

Total RNA was extracted from BMSCs and femoral head tissues using TRIzol Reagent. The specific primers sequences are listed in Table 1. All qRT-PCR analyses were performed by the Light-Cycler® 480 Real-time PCR System (Roche). U6 snRNA and β-actin mRNA levels were used for normalization. The thermal cycling conditions were as follows: 10 min at 95 °C and 40 cycles of 10 s at 95 °C and 60 s at 60 °C. Data were analyzed by the relative quantification ($2^{-\triangle\triangle}$CT) method. The fold change in transcript level was calculated using ΔΔCT normalized to control (Brazvan et al., 2016; Fathi et al., 2020).

2.9. Western blot analysis

Total protein was isolated from cultured cells by lysing with lysis buffer containing phenylmethylsulfonyl fluoride (PMSF) on ice. The femoral head was placed in liquid nitrogen and ground followed by lysis using the above lysis buffer. After lysis, the total protein concentration was determined using a Bio-Rad protein assay system (Bio-Rad, Hercules, CA, USA), and 60 μg of total protein was electrophoresed on 12% SDS polyacrylamide gels followed by transfer to a PVDF membrane (Millipore). Membranes were blocked with 5% nonfat milk solution at room temperature for 2 h and then incubated with anti-BMP-2 (Abcam, ab14933, USA, dilution 1:500), anti-BMP-4 (Abcam, ab39973, USA, dilution 1:500), anti-Runx2 (Abcam, ab76956, USA, dilution 1:200), anti-phosphorylated-Smad5 (p-Smad5, Abcam, ab92698, USA, dilution 1:200), anti-Smad5 (Abcam, ab40771, USA, dilution 1:1000), anti-Wnt1 (Abcam, ab15251, USA, dilution 1:100), anti-β-catenin (Abcam, ab68183, USA, dilution 1:500) and GAPDH antibodies for 2 h at 37 °C. The membranes were then washed three times and incubated with horseradish peroxidase-conjugated secondary antibodies for 1 h at room temperature. The membranes were then incubated with ECL solution (Millipore, Darmstadt, Germany), and the protein bands were scanned and quantified (Brazvan et al., 2016; Fathi et al., 2020). The relative band intensity was assessed as the ratio of the gray value of each protein to that of the corresponding GAPDH.

2.10. Animal model establishment and grouping

Animal modeling procedures were performed on male Wistar rats weighing 200–250 g. Forty-five rats were housed in a standard animal care room (12-h light/dark cycle; 22–26 °C; humidity, 37%-42%) with free access to food and water during the study. After adaptive feeding for 1 week, a rat model of femoral head necrosis was established. The experimental studies were approved by the Institutional Animal Care and Use Committee of Guangxi University of Chinese Medicine (Approval No: DW-20190829–031).

Thirty-nine rats were included in the model group and modeled with lipopolysaccharide (LPS) and methylprednisolone. The rats were given two intraperitoneal injections of 20 μg/kg LPS (*Escherichia coli* 055:B5, Sigma, USA) on days 0 and 1 at a time interval of 24 h. After 24 h, the rats received three intramuscular injections of 40 mg/kg methylprednisolone sodium succinate (Pfizer Pharmaceutical, China) on days 3, 4 and 5 at a time interval of 24 h (Dong et al., 2015). Six rats were included in the blank control group and were subjected to the same injection procedure but with an equal volume of saline. In total, 36 rats were successfully modeled and grouped into the following 6 groups: the model group (injected with an equal volume of saline), the BMSC group (injected with 1×10^6 BMSCs), the miR-23a-NC group (injected with

Table 1
Primers used for qRT-PCR analysis.

Gene name	Prime name	Primers (5′ to 3′)	Length
GAPDH	Forward	TGACAACTTTGGCATCGTGG	78
	Reverse	GGGCCATCCACAGTCTTCTG	
BMP-2	Forward	GGACGTCCTCAGCGAGTTT	106
	Reverse	CAGGTCGAGCATATAGGGGG	
BMP-4	Forward	CAGGGCCAACATGTCAGGAT	147
	Reverse	GTGATGCTTGGGACTACGCT	
Runx2	Forward	GCCTTCAAGGTTGTAGCCCT	133
	Reverse	TGAACCTGGCCACTTGGTTT	
Samd5	Forward	TGTTGGGCTGGAAACAAGGT	94
	Reverse	GTGACACACTTGCTTGGCTG	
Wnt1	Forward	CAACATCGATTTCGGTCGCC	79
	Reverse	CATGAGGAAGCGTAGGTCCC	
β-catein	Forward	ACTCCAGGAATGAAGGCGTG	109
	Reverse	GAACTGGTCAGCTCAACCGA	
miR-23a-3p	RT	GTCGTATCCAGTGCGTGTCGTGGAGTCGGCAATTGCACTGGATACGACGGAAATCC	61
	Forward	CGGATCACATTGCCAGGG	
	Reverse	CAGTGCGTGTCGTGGAGT	

1×10^6 miR-23a-3p-negative BMSCs), the miR-23a-NC + icariin group (injected with 1×10^6 miR-23a-3p-negative BMSCs and gavaged with 200 mg/kg icariin), the miR-23a inhibitor group (injected with 1×10^6 miR-23a-3p-inhibitor BMSCs) and the miR-23a inhibitor + icariin group (injected with 1×10^6 miR-23a-3p-inhibitor BMSCs and gavaged with 200 mg/kg icariin). After successful modeling, the rats were anesthetized, and 200 μL of BMSCs (1×10^6), miR-23a-3p-negative BMSCs (1×10^6) or miR-23a-3p-inhibitor BMSCs (1×10^6) was injected into the femur bone marrow cavity using a microsyringe. Postoperative intraperitoneal injection of antibiotics was performed to prevent infection. The above intragastric administration was prepared once a day for a total of 28 days. On the 7th, 14th and 28th days, blood was collected from the rats, centrifuged and stored at −20 °C. The rats were then subjected to digital radiography (DR) examination (Goodsee, #GDA32-02, China) and sacrificed, and bilateral femurs were collected for HE staining, RT-PCR and Western blotting.

2.11. Hematoxylin-eosin (HE) staining

Pathological changes in the femoral head were detected by HE staining (Zhang et al., 2019). After fixation and decalcification, <0.5 cm × 0.5 cm × 0.1 cm of tissue was removed. The sections were fixed, embedded and subjected to HE staining. The 5-μm sections were soaked in water, differentiated in hydrochloric acid ethanol for 30 s and rinsed in water for 5 min. The sections were then recovered in ammonia water for 10 min and stained with eosin for 2 min. The sections were dehydrated via alcohol, cleaned three times with xylene and sealed with neutral balsam. Finally, images were acquired at 400x magnification (CX71, Olympus Corporation, Tokyo, Japan).

2.12. ELISA

Rat tail vein blood was collected and preserved in a nonanticoagulant tube. After standing at room temperature for 30 min and centrifugation at 2000 r/min for 10 min, the upper serum was collected and stored at −80 °C. ELISA kits (Cloud Clone, Wuhan, China) were used to determine serum levels of ACP-5, BAP, NXTI, CTXI and OC according to the manufacturer's instructions (Brazvan et al., 2016).

2.13. Statistical analyses

The results were expressed as the mean ± SD. All experiments were performed with randomization of group assignment via allocation concealment, blinding of operators, blinding of measurements and blinding of analyses. When only two groups were compared, a Student's *t*-test was used. Multiple comparisons were evaluated by one-way or two-way Anova (with repeated measures when appropriate) followed by Tukey-Kramer tests or Bonferroni corrections. Outcomes were considered statistically significant with two-tailed $P < 0.05$.

3. Results

3.1. Characteristics and osteogenic differentiation of BMSCs

After isolation of the BMSCs (Fig. 1A), flow cytometry identified the purity of BMSCs using a fluorescently labeled antibody. As shown in Fig. 1B, alizarin red staining verified that BMSCs were induced into osteoblasts after 21 days of osteogenic induction. As shown in Fig. 1C, the percentages of CD29-PE-, CD44-FITC-, CD34-FITC- and CD45-PE-positive BMSCs were 94.87%, 98.98%, 0.45% and 0.16%, respectively. Immunophenotypic studies have shown that cultured BMSCs are CD29- and CD44-positive but CD34- and CD45-negative (Kim et al., 2011; Jiang et al., 2010). BMSCs can be induced into osteoblasts, and alizarin red staining is used for the identification of osteogenic ability (Li et al., 2019). Therefore, these data showed that the isolated BMSCs were BMSCs and could be used for subsequent experiments.

3.2. Icariin treatment/miR-23a-3p knockdown increases ALP activity and BMSC viability via the BMP-2/Smad5/Runx2 and WNT/β-catenin pathways in BMSCs

After 9 days of induction with the same serum concentration (5% and 10%), the ALP activity of the icariin-containing serum group was significantly higher than that of the icariin-free serum group. Treatment with the various concentrations of icariin-containing serum (0%, 2.5%, 5% and 10%) indicated that the ALP activity was upregulated in a dose-dependent manner (Fig. 2A). Therefore, we selected 10% icariin-containing serum for the subsequent BMSC culture. After icariin treatment or miR-23a-3p knockdown (markedly decreased miR-23a-3p level; Supplemental Fig. 1B), ALP activity was significantly upregulated ($P < 0.05$), and combined icariin treatment and miR-23a-3p knockdown increased ALP activity compared to single icariin treatment or miR-23a-3p knockdown (Fig. 2B, $P < 0.05$).

As shown in Fig. 2C, BMSC viability in the icariin and miR-23a-3p inhibitor groups was significantly higher than that in the icariin-free serum (miR-23a-NC) group ($P < 0.05$). Surprisingly,

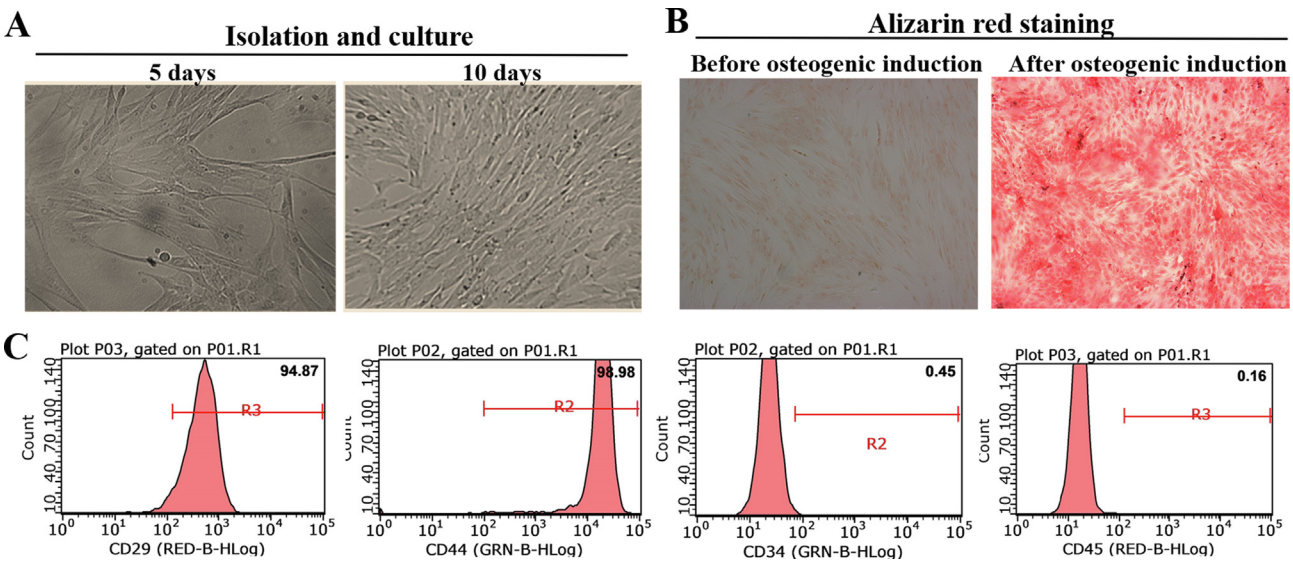

Fig. 1. Images of isolated BMSCs (A), osteogenic differentiation of BMSCs (B) and flow cytometric identification (C). Flow cytometry using a fluorescently labeled antibody was used to identify the purity of the BMSCs.

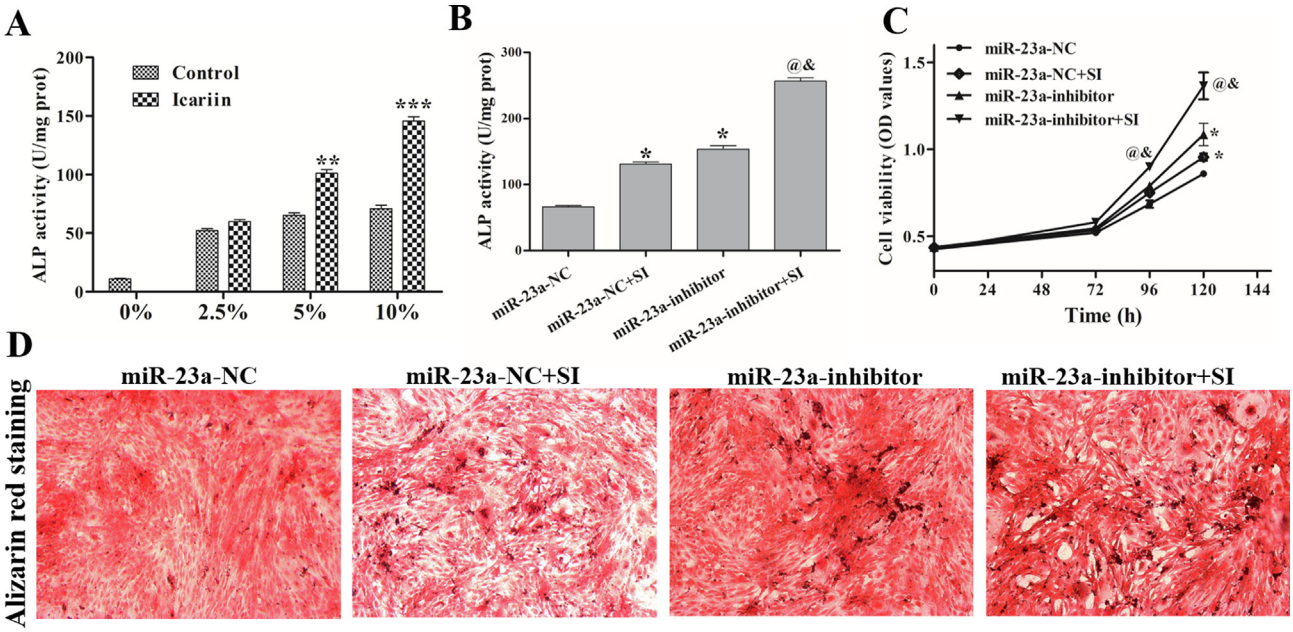

Fig. 2. Icariin treatment/miR-23a-3p knockdown promotes ALP activity and induces the expression of BMP-2, BMP-4, Runx2, p-Smad5, Wnt1 and β-catenin in BMSCs. (A) BMSCs were induced with different concentrations of icariin-containing serum (0%, 2.5%, 5% and 10%) for 9 days, and the ALP activity was measured. Data are represented as the means ± SD (n = 3). $^{**}P < 0.01$ and $^{***}P < 0.001$ vs. corresponding control group. (B) ALP activity in different groups. (C) Cell viability in different groups. (D) Alizarin red staining was performed to detect the osteogenic differentiation of BMSCs. Data are represented as the means ± SD (n = 3). $^{*}P < 0.05$ vs. miR-23a-NC group. $^{@}P < 0.05$ vs. miR-23a-NC + SI group. $^{\&}P < 0.05$ vs. miR-23a-inhibitor group.

compared to the single icariin treatment or miR-23a-3p inhibitor group, BMSC viability was significantly increased in the combined icariin treatment and miR-23a-3p knockdown group ($P < 0.05$). Additionally, Alizarin red staining showed that icariin treatment/miR-23a-3p knockdown induced osteogenic differentiation of BMSCs, and combined icariin treatment and miR-23a-3p knockdown significantly induced osteogenic differentiation of BMSCs compared to single icariin treatment or miR-23a-3p knockdown (Fig. 2D, $P < 0.05$).

RT-PCR and Western blot analyses were used to detect the mRNA and protein expression levels, respectively, of BMP-2, BMP-4, Runx2, p-Smad5/Smad5, Wnt1 and β-catenin. After icariin treatment or miR-23a-3p knockdown, the protein and mRNA levels of BMP-2, BMP-4, Runx2, Wnt1 and β-catenin as well as the phosphorylation level of p-Smad5 were significantly higher than those in the miR-23a-NC control group ($P < 0.05$). In addition, after combined icariin treatment and miR-23a-3p knockdown, the mRNA and protein levels of BMP-2, BMP-4, Runx2, p-Smad5/Smad5, Wnt1 and β-catenin were markedly increased compared to those in the miR-23a-NC + SI and miR-23a inhibitor groups (Fig. 3A–C).

TargetScan was used to predict the target gene of miR-23a-3p, which predicted that Runx2 may contain a putative binding site with miR-23a-3p. The luciferase activity results demonstrated that cotransfection of the luciferase reporter plasmid containing

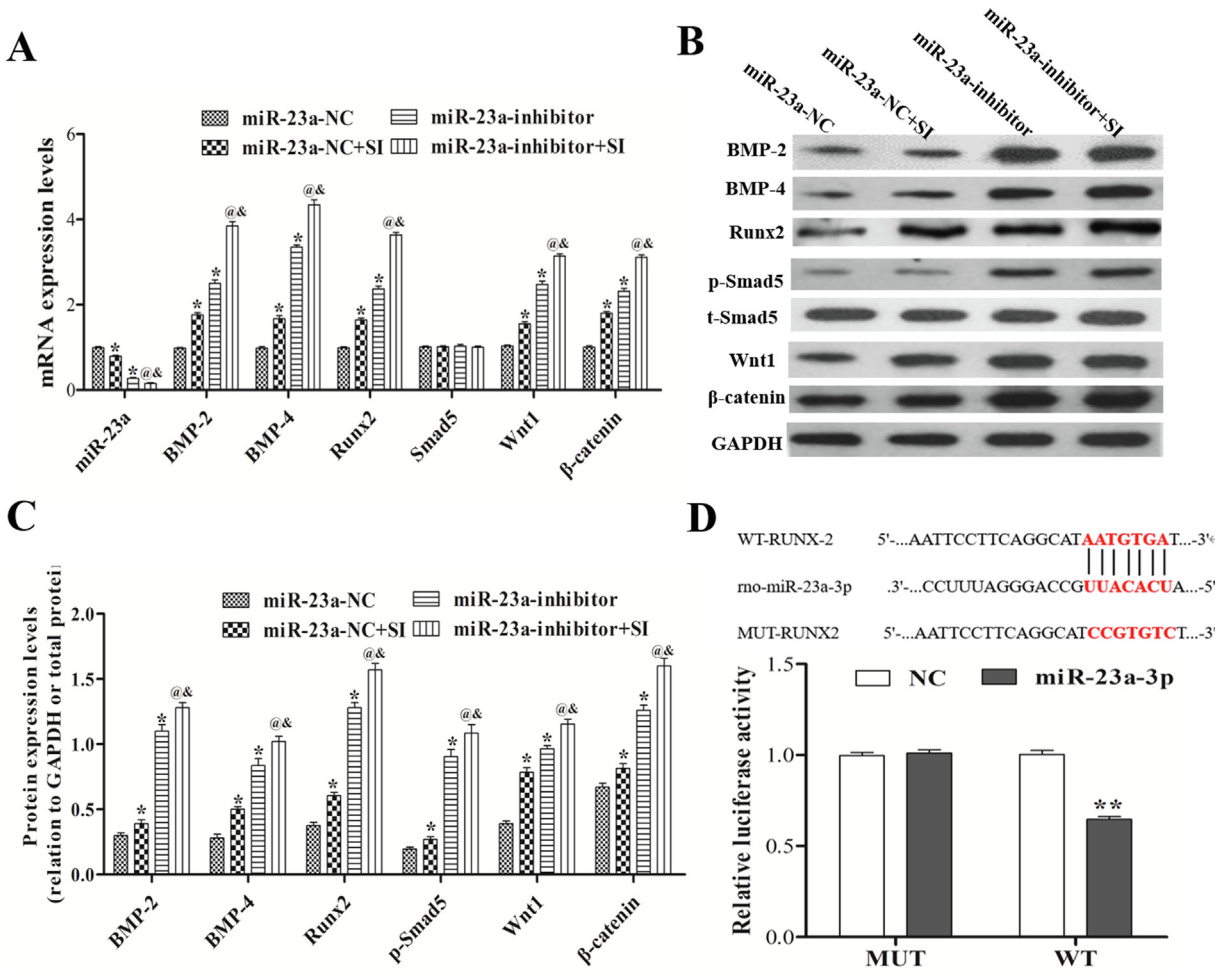

Fig. 3. Icariin treatment/miR-23a-3p knockdown induces the expression of BMP-2, BMP-4, Runx2, p-Smad5, Wnt1 and β-catenin in BMSCs. (A) RT-PCR was used to detect the expression of BMP-2, Runx2, Smad5, Wnt1 and β-catenin mRNA. (B and C) Western blotting was used to detect the protein expression of BMP-2, BMP-4, Runx2, p-Smad5, Wnt1 and β-catenin. (D) Dual-luciferase reporter assay was used to verify the relationship of miR-23a-3p and Rnux2. Data are represented as the means ± SD (n = 3). $^{*}P < 0.05$ vs. its miR-23a-NC group. $^{@}P < 0.05$ vs. miR-23a-NC + SI group. $^{\&}P < 0.05$ vs. miR-23a-inhibitor group.

Runx2-Wild type (WT) with the miR-23a-3p inhibitor significantly decreased the reporter activity compared to the negative control in BMSCs ($P < 0.05$), while the miR-23a-3p inhibitor did not affect the luciferase activity of the Runx2 mutant (MUT). These results demonstrated that miR-23a-3p directly targets Runx2 in BMSCs (Fig. 3D).

These results revealed that icariin treatment/miR-23a-3p knockdown increases ALP activity and BMSC viability, thereby promoting the osteogenic differentiation of BMSCs via the BMP-2/Smad5/Runx2 and WNT/β-catenin pathways.

3.3. Icariin treatment/miR-23a-3p knockdown improves osteonecrosis of the femoral head

In the blank group, HE staining showed (Fig. 4) that the structure of the femoral head was complete and that the chondrocytes and trabecular bone were normal. After ONFH modeling, the normal structures of the femoral head changed, and the number of cartilage and chondrocytes increased compared to the blank group. In addition, ONFH modeling resulted in many empty lacunae compared to the blank group. After injection of BMSCs or miR-23a-NC BMSCs, chondrocytes proliferation was observed around the medulla. After icariin treatment, the structure of the cartilaginous layer was not complete, and the number of cartilage and chondrocytes increased compared to the model group. After knockdown of miR-23a-3p (Supplemental Fig. 1C), the structure of the cartilaginous layer was complete, and the number of cartilage and chondrocytes significantly increased compared to the model group. After combined icariin treatment and miR-23a-3p knockdown, the number of cartilage and chondrocytes significantly increased, and the structure of the cartilaginous layer was complete and trended to normal. HE staining showed that icariin induces new bone formation of the femur head.

DR of the femur head showed early osteonecrosis in the rat ONFH model, and the necrotic area was predominantly located in cancellous bone and the chondral region. In the ONFH model, the femur head presented shrinkage and partial collapse, and bone trabeculae appeared thinner. After icariin treatment or miR-23a-3p

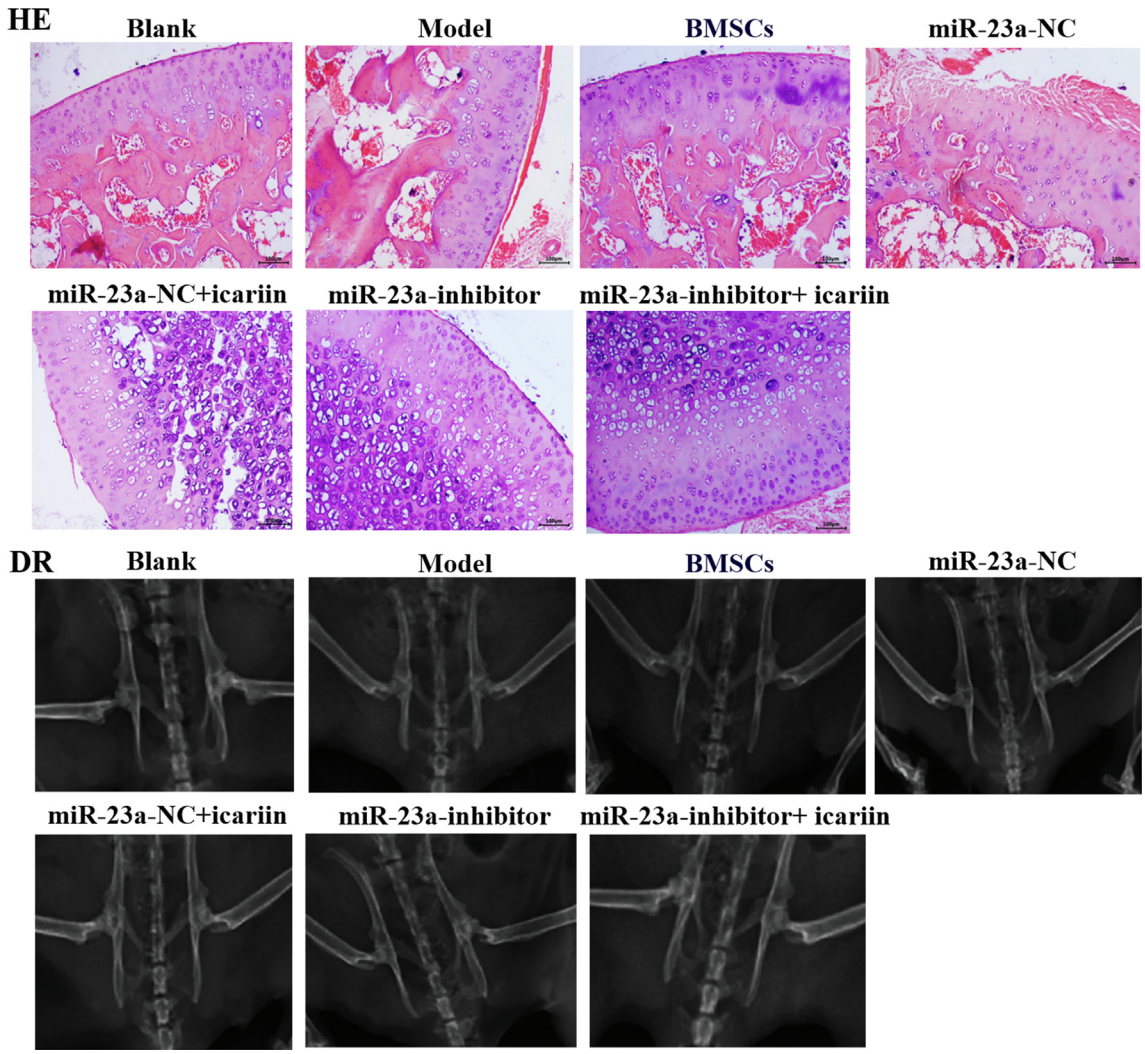

Fig. 4. Icariin treatment/miR-23a-3p knockdown improves osteonecrosis of the femoral head. (A) HE staining was used to observe the morphological changes of the femoral head. (B) Digital radiography (DR) was used to observe the femoral head after 28 treatments.

knockdown, necrosis of the femur head was partially repaired. After combined icariin treatment and miR-23a-3p knockdown, the cartilage layer and bone trabeculae appeared thicker. The DR images (Fig. 4) showed that icariin treatment/miR-23a-3p knockdown accelerates the repair of the femur head.

Thus, HE staining and DR indicated that icariin treatment/miR-23a-3p knockdown induces bone formation and accelerates the repair of the femur head, ultimately improving osteonecrosis of the femoral head.

3.4. Icariin treatment/miR-23a-3p knockdown activates the BMP-2/Smad5/Runx2 and WNT/β-catenin pathways in the ONFH model

RT-PCR and Western blot analyses (Fig. 5) detected the mRNA and protein expression levels, respectively, of BMP-2, BMP-4, Runx2, p-Smad5/Smad5, Wnt1 and β-catenin. Compared to the blank control group, the mRNA and protein expression levels of BMP-2, BMP-4, Runx2, p-Smad5/Smad5, Wnt1 and β-catenin in the ONFH model group were significantly decreased, and their levels were significantly lower than those in BMSCs group and miR-23a-NC group ($P < 0.05$). After icariin treatment or miR-23a-3p knockdown, the mRNA and protein levels of BMP-2, BMP-4, Runx2, Wnt1 and β-catenin as well as the phosphorylation level of p-Smad5 were significantly higher than those in the miR-23a-NC group ($P < 0.05$). In addition, after combined icariin treatment and miR-23a-3p knockdown, the mRNA and protein levels of BMP-2, BMP-4, Runx2, p-Smad5/Smad5, Wnt1 and β-catenin were significantly increased compared to those in the miR-23a-NC + icariin and miR-23a inhibitor groups. These data showed that icariin treatment/miR-23a-3p knockdown activates the BMP-2/Smad5/Runx2 and WNT/β-catenin pathways in the ONFH model.

3.5. Icariin treatment/miR-23a-3p knockdown regulates the levels of bone formation- and bone resorption-specific markers in ONFH model rats

At 7 days, 14 days and 28 days after icariin treatment/miR-23a-3p knockdown, we detected the levels of bone formation- and bone resorption-specific markers. Fig. 6 shows that the levels of ACP-5, BAP, NTXI, CTXI and OC in icariin-treated and miR-23a-3p knockdown rats were significantly higher than those in ONFH model rats. Surprisingly, compared to the icariin treatment/miR-23a-3p knockdown group, the levels of ACP-5, BAP, NTXI, CTXI and OC in the miR-23a-inhibitor + icariin group were significantly increased. In addition, compared to the corresponding 7-day data, the levels of ACP-5, BAP, NTXI, CTXI and OC on days 14 and 28 were significantly increased. These results revealed that icariin treatment/

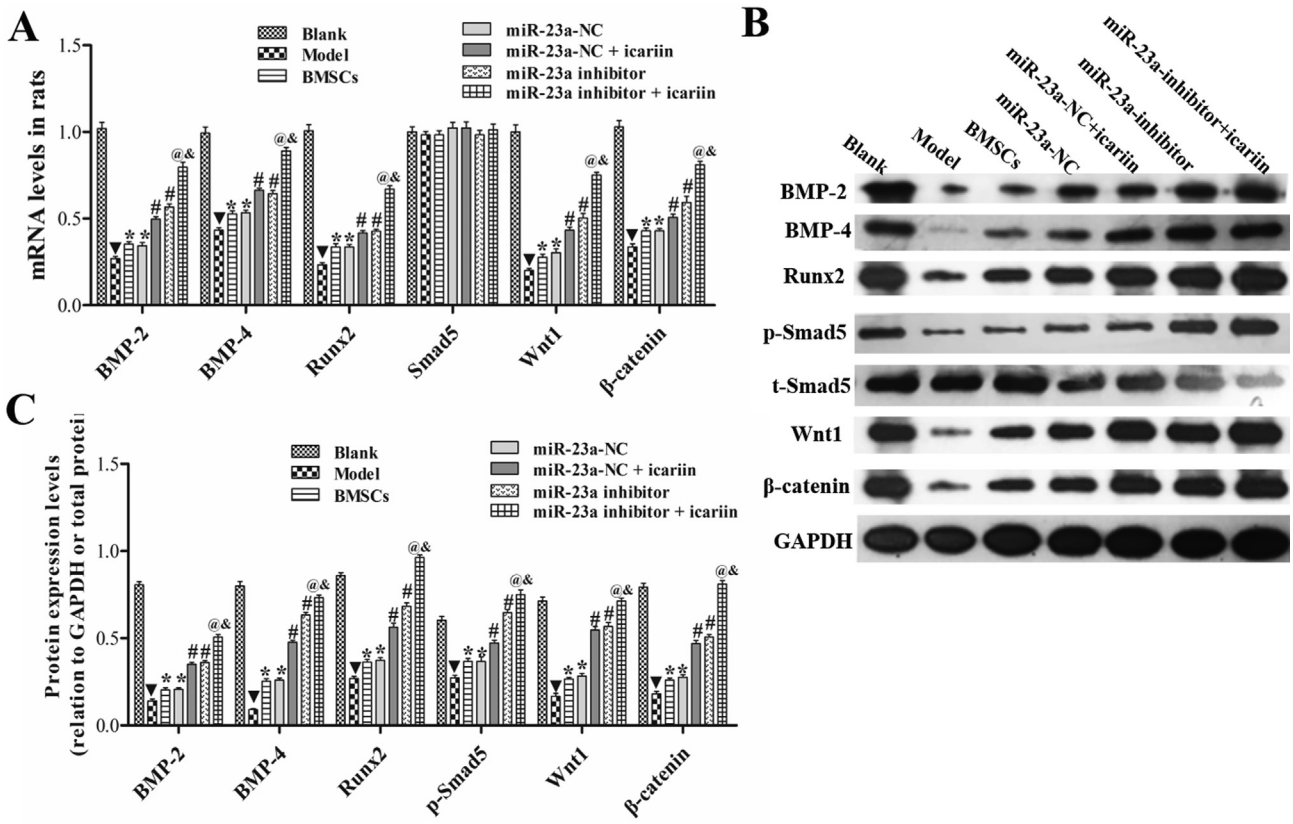

Fig. 5. Icariin treatment/miR-23a-3p knockdown induces the expression of BMP-2, BMP-4, Runx2, p-Smad5, Wnt1 and β-catenin in the ONFH model. (A) RT-PCR was used to detect the expression of BMP-2, Runx2, Smad5, Wnt1 and β-catenin mRNA. (B and C) Western blotting was used to detect the protein expression of BMP-2, BMP-4, Runx2, p-Smad5, Wnt1 and β-catenin. Data are represented as the means ± SD (n = 6). $^{▼}P < 0.05$ vs. blank group. $^{*}P < 0.05$ vs. model group. $^{\#}P < 0.05$ vs. miR-23a-NC group. $^{@}P < 0.05$ vs. miR-23a-NC + icariin group. $^{\&}P < 0.05$ vs. miR-23a-inhibitor group.

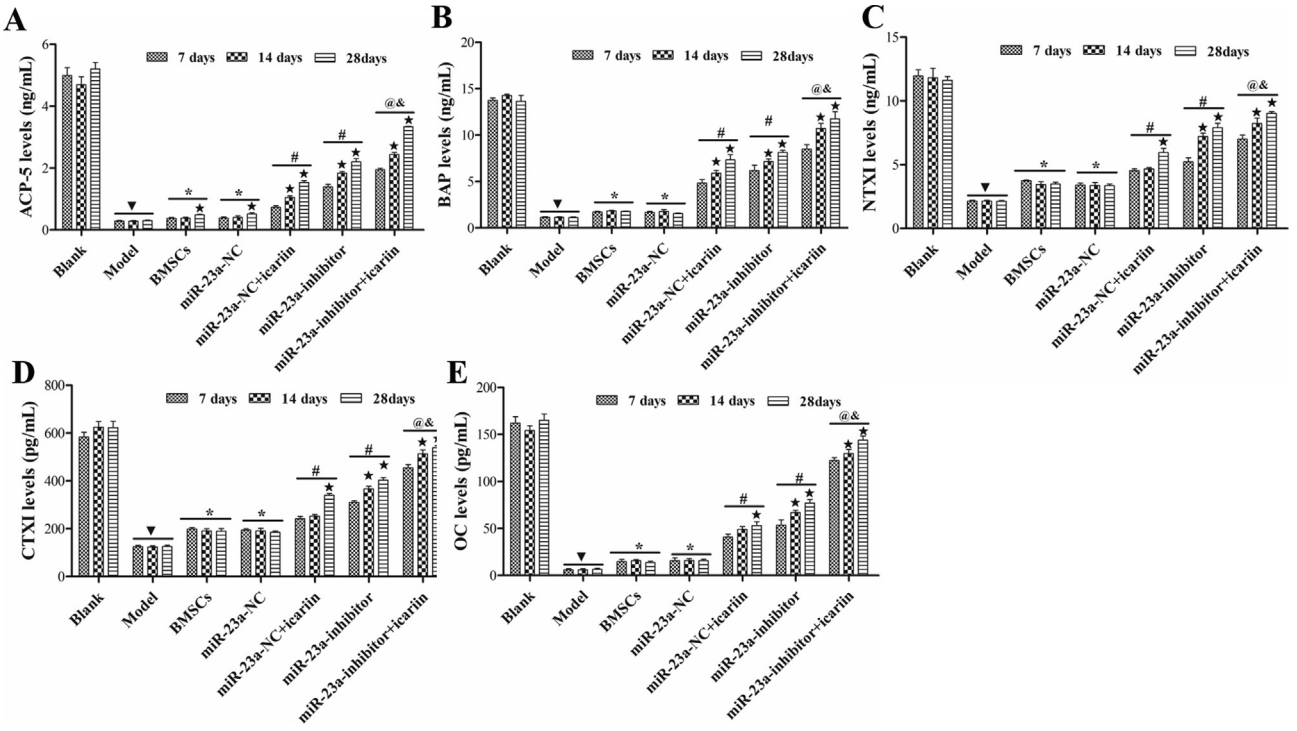

Fig. 6. Icariin treatment/miR-23a-3p knockdown increases the levels of ACP-5 (A), BAP (B), NTXI (C), CTXI (D) and OC (E) in the ONFH model. Data are represented as the means ± SD (n = 6). $^{▼}P < 0.05$ vs. blank group. $^{★}P < 0.05$ vs. corresponding 7 days group. $^{*}P < 0.05$ vs. model group. $^{\#}P < 0.05$ vs. miR-23a-NC group. $^{@}P < 0.05$ vs. miR-23a-NC + icariin group. $^{\&}P < 0.05$ vs. miR-23a-inhibitor group.

miR-23a-3p knockdown accelerates bone formation and bone resorption in a time-dependent manner.

4. Discussion

ONFH is a disease of mesenchymal or bone cells that is common in people who take hormones and ingest alcohol for a long time, and it can cause femoral head collapse and even require total hip replacement (Zhang et al., 2010). BMSCs are multipotent cells that can differentiate into osteoblastic cells under the appropriate conditions (Kreke et al., 2005). Clinically, implantation of BMSCs has been used as a cellular therapeutic option for the treatment of ONFH, and implanted BMSCs can differentiate into osteoblasts (Ji et al., 2008). Traditional Chinese medicine promotes osteoinduction in the repair of ONFH. Huo Xue Tong Luo capsule (HXTL capsule) promotes osteogenesis in rat MSCs (B. Fang et al., 2019). In the present study, we successfully isolated rat BMSCs and found that icariin treatment/miR-23a-3p knockdown induced BMSC viability and osteogenic differentiation via the BMP-2/Smad5/Runx2 and WNT/β-catenin pathways in vitro. Furthermore, implantation of BMSCs into the femoral head with combined icariin treatment and miR-23a-3p knockdown accelerated osteogenic differentiation and improved ONFH (HE staining and DR). In summary, our study showed that icariin may be developed as an ONFH treatment drug and that miR-23a-3p may be a target for ONFH treatment.

Chinese herbal medicines are considered economical and safe because they are less toxic, and they have been used to cure different diseases, including ONFH and osteoporosis (Wang et al., 2018; Yu et al., 2019; Cheng et al., 2014). Osteoblast proliferation and osteogenic differentiation are the keys to the recovery of ONFH (Zhao et al., 2010). ALP, a marker enzyme involved in metabolism and regeneration of bone and other mineralized tissues, is a key molecule that determines the degree of bone mineralization (Huang et al., 2019; Halling Linder et al., 2017). Genistein stimulates the proliferation and osteoblastic differentiation of mouse BMSCs, and it promotes bone anabolism (Pan et al.,2005). Cao et al. found that icariin promotes osteogenic differentiation through increased mRNA expression of BMP-2 in BMSCs (Cao et al., 2012). Zhao et al. found that icariin exerts its potent osteogenic effect through induction of Runx2 expression, production of BMP-4 and activation of BMP signaling (Zhao et al., 2008). Cajan leaves combined with BMSCs promote vascular endothelial growth factor (VEGF) expression and improves ONFH repair (Shi, et al., 2014). Our results supported this previous finding as they showed that icariin promoted ALP (BAP) levels in BMSCs and ONFH rats. Furthermore, icariin promoted bone biochemical markers (ACP-5, BAP, NTXI, CTXI and OC) in the serum of ONFH rats. These data indicated that icariin promotes osteogenic differentiation of BMSCs and stimulates bone formation in rats, thereby improving ONFH.

Increasing evidence has indicated that miRNAs play a vital role in the development of various bone diseases. miRNA microarray chip analysis has revealed that 22 miRNAs are upregulated and 17 miRNAs are downregulated in nontraumatic ONFH samples (Wu et al., 2015; Wang et al., 2014). Among all the miRNAs in ONFH, miR-23a-3p has been reported to be upregulated in both serum and bone tissue, and the upregulation of miR-23a-3p may lead to the downregulation of Runx2, which in turn results in less new bone formation of the trabecular bone (Ramírez-Salazar et al., 2018; Kelch et al., 2017). In contrast, inhibiting miR-23a-3p enhances the osteogenic differentiation of BMSCs (Li et al., 2016). miR-23a downregulation and icariin have the same effect on hBMSCs in vitro as both promote hBMSC osteogenic differentiation and activate the Wnt/β-catenin signaling pathway (Xu et al., 2021). In the present study, RT-PCR analysis indicated that miR-23a-3p was markedly upregulated in the ONFH model, which agreed with previous studies. Interestingly, TargetScan predicted that Runx2 might be a target of miR-23a-3p. Luciferase assays demonstrated that Runx2 was directly targeted by miR-23a-3p, and their expression was negatively correlated. Therefore, we identified miR-23a-3p as a negative regulator of BMSC osteogenic differentiation. Compared to the control group, the icariin, miR-23a-3p inhibitor and icariin + miR-23a-3p inhibitor groups significantly promoted and enhanced the mRNA and protein expression of BMP-2, BMP-4, Runx2, p-Smad5, Wnt1 and β-catenin with the icariin + miR-23a-3p inhibitor group resulting in the greatest enhancement of expression. Therefore, icariin may promote osteogenic differentiation by downregulating miR-23a-3p.

The BMP 2/Smad5/Runx2 and Wnt/β-catenin pathways are the most important pathways in osteoblast proliferation and differentiation. Bone morphogenetic proteins (BMPs) trigger intracellular signaling and activate Smad complexes that regulate the transcription of BMP-responsive genes, including Runx2 (Leboy et al., 2001). Several studies have reported that BMP-2, BMP-4 and Runx2 are osteogenic markers of osteogenesis (Doecke et al., 2006). Zhang et al. found that icariin promotes bone formation by upregulating the BMP2/Runx2 and OPG/RANKL pathways under high local concentrations of vancomycin treatment (Zhang et al., 2017). Robinson et al. found that upregulation of the Wnt/β-catenin signaling pathway is required for bone formation in response to mechanical loading (Robinson et al., 2016). Icariin promotes hBMSC osteogenesis in vitro via activation of the Wnt/β-catenin signaling pathway (Xu et al., 2021). Our previous study demonstrated that icariin activates the WNT1/β-catenin osteogenic signaling pathway in a fracture model (Zhang et al., 2020). In the present study, we found that icariin treatment/miR-23a-3p knockdown upregulated the levels of BMP-2, BMP-4, Runx2, p-Smad5, Wnt1 and β-catenin in BMSCs and ONFH model rats, thereby activating the BMP 2/Smad5/Runx2 and WNT1/β-catenin pathways. In addition to previous research, the present study demonstrated that icariin promotes osteogenic differentiation via activation of the BMP 2/Smad5/Runx2 and Wnt/β-catenin pathways.

5. Conclusion

Icariin promotes BMSC viability and osteogenic differentiation, thereby improving ONFH via decreasing miR-23a-3p levels and regulating the BMP-2/Smad5/Runx2 and WNT/β-catenin pathways. Icariin plays a positive role in miR-23a-3p-mediated osteogenic differentiation and cell viability of BMSCs. Therefore, icariin may be developed as an ONFH treatment drug.

Declaration of Competing Interest

The authors declare that they have no known competing financial interests or personal relationships that could have appeared to influence the work reported in this paper.

Acknowledgement

This work was supported by the National Natural Science Foundation of China (grant number 81760796), Guangxi Natural Science Foundation (grant number 2020GXNSFBA159053), Guangxi University Young Teachers' Basic Ability Improvement Project (grant number 2019KY0352), and the High-level Talent Team Cultivation Project of "Qi Huang" of Guangxi University of Traditional Chinese Medicine (grant number 04B1804804).

Appendix A. Supplementary material

Supplementary data to this article can be found online at https://doi.org/10.1016/j.jsps.2021.10.009.

References

Brazvan, B., Farahzadi, R., Mohammadi, S.M., Saheb, S.M., Shanehbandi, D., Schmied, L., Rad, J.S., Darabi, M., Charoudeh, H.N., 2016. Key Immune Cell Cytokines Affects the Telomere Activity of Cord Blood Cells In vitro. Adv. Pharm. Bull. 6 (2), 153–161.

Cao, H., Ke, Y., Zhang, Y., Zhang, C.J., Qian, W., Zhang, G.L., 2012. Icariin stimulates MC3T3-E1 cell proliferation and differentiation through up-regulation of bone morphogenetic protein-2. Int. J. Mol. Med. 29 (3), 435–439.

Cao, X., Zhu, N.a., Zhang, Y., Chen, Y., Zhang, J., Li, J., Hao, P., Gao, C., Li, L.i., 2020. Y-box protein 1 promotes hypoxia/reoxygenation- or ischemia/reperfusion-induced cardiomyocyte apoptosis via SHP-1-dependent STAT3 inactivation. J. Cell Physiol. 235 (11), 8187–8198.

Cheng, K., Ge, B.F., Chen, K.M., Zhen, P., Zhou, J., Ma, X.N., Song, P., Ma, H.P., 2014. Oral medication of icariin enhances peak bone mineral density and bone quality in rats. Chin. J. Osteopor. 20, 120–124.

Dai, J., Li, Y., Zhou, H., Chen, J., Chen, M., Xiao, Z., 2013. Genistein promotion of osteogenic differentiation through BMP2/SMAD5/RUNX2 signaling. Int. J. Biol. Sci. 9 (10), 1089–1098.

Dai, Y., Zheng, C., Li, H., 2019. Inhibition of miR-23a-3p promotes osteoblast proliferation and differentiation. J. Cell. Biochem. https://doi.org/10.1002/jcb.29497.

Doecke, J.D., Day, C.J., Stephens, A.SJ., Carter, S.L., van Daal, A., Kotowicz, M.A., Nicholson, G.C., Morrison, N.A., 2006. Association of functionally different RUNX2 P2 promoter alleles with BMD. J. Bone. Miner. Res. 21 (2), 265–273.

Dong, Y., Li, T., Li, Y., Ren, S., Fan, J., Weng, X., 2017. MicroRNA-23a-3p inhibitor decreases osteonecrosis incidence in a rat model. Mol. Med. Rep. 16 (6), 9331–9336. https://doi.org/10.3892/mmr.2017.7808.

Dong, Y., Li, Y., Huang, C., Gao, K., Weng, X., 2015. Systemic application of teriparatide for steroid induced osteonecrosis in a rat model. BMC Musculoskelet. Disord. 16, 163.

Fathi, E., Farahzadi, R., Javanmardi, S., Vietor, I., 2020. L-carnitine Extends the Telomere Length of the Cardiac Differentiated CD117 $^{+}$ - Expressing Stem Cells. Tissue Cell. 67, 101429. https://doi.org/10.1016/j.tice:2020.101429.

Fang, S.H., Li, Y.F., Jiang, J.R., Chen, P., 2019a. Relationship of alpha2-Macroglobulin with Steroid-Induced Femoral Head Necrosis: A Chinese Population-Based Association Study in Southeast China. Orthop. Surg. 11 (3), 481–486.

Fang, B., Li, Y., Chen, C., Wei, Q., Zheng, J., Liu, Y., He, W., Lin, D., Li, G., Hou, Y., Xu, L., 2019b. Huo Xue Tong Luo capsule ameliorates osteonecrosis of femoral head through inhibiting lncRNA-Miat. J. Ethnopharmacol. 238, 111862. https://doi.org/10.1016/j.jep.2019.111862.

Farahzadi, R., Fathi, E., Vietor, I., 2020. Mesenchymal Stem Cells Could Be Considered as a Candidate for Further Studies in Cell-Based Therapy of Alzheimer's Disease via Targeting the Signaling Pathways. ACS Chem. Neurosci. 11 (10), 1424–1435.

Farahzadi, R., Mesbah-Namin, S.A., Zarghami, N., Fathi, E., 2016. L-carnitine Effectively Induces hTERT Gene Expression of Human Adipose Tissue-derived Mesenchymal Stem Cells Obtained from the Aged Subjects. Int J Stem Cells. 9 (1), 107–114.

Gu, H., Boonanantanasarn, K., Kang, M., Kim, I., Woo, K.M., Ryoo, H.M., Baek, J.H., 2018. Morinda citrifolia Leaf Extract Enhances Osteogenic Differentiation Through Activation of Wnt/β-Catenin Signaling. J. Med. Food. 21 (1), 57–69. https://doi.org/10.1089/jmf.2017.3933.

Halling Linder, C., Ek-Rylander, B., Krumpel, M., Norgård, M., Narisawa, S., Millán, J. L., Andersson, G., Magnusson, P., 2017. Bone Alkaline Phosphatase and Tartrate-Resistant Acid Phosphatase: Potential Co-regulators of Bone Mineralization. Calcif. Tissue. Int. 101 (1), 92–101.

Huang, X., Wang, X., Zhang, Y., Shen, L., Wang, N., Xiong, X., Zhang, L.i., Cai, X., Shou, D., 2019. Absorption and utilisation of epimedin C and icariin from Epimedii herba, and the regulatory mechanism via the BMP2/ Runx2 signalling pathway. Biomed. Pharmacother. 118, 109345. https://doi.org/10.1016/j.biopha.2019.109345.

Huang, Z., Fu, F., Ye, H., Gao, H., Tan, B., Wang, R., Lin, N., Qin, L., Chen, W., 2020. Chinese herbal Huo-Gu Formula for treatment of steroid-associated osteonecrosis of femoral head: a 14-years follow-up of convalescent SARS patients. J. Orthop. Transl. 23, 122–131.

Ji, W.F., Ding, W.H., Ma, Z.C., Li, J., Tong, P.J., 2008. Three-tunnels core decompression with implantation of bone marrow stromal cells (bMSCs) and decalcified bone matrix (DBM) for the treatment of early femoral head necrosis. Zhongguo. Gu. Shang. 21 (10), 776–778.

Jiang, T.S., Cai, L., Ji, W.Y., Hui, Y.N., Wang, Y.S., Hu, D., Zhu, J., 2010. Reconstruction of the corneal epithelium with induced marrow mesenchymal stem cells in rats. Mol. Vis. 16, 1304–1316.

Karasuyama, K., Yamamoto, T., Motomura, G., Sonoda, K., Kubo, Y., Iwamoto, Y., 2015. The role of sclerotic changes in the starting mechanisms of collapse: A histomorphometric and FEM study on the femoral head of osteonecrosis. Bone. 81, 644–648.

Kelch, S., Balmayor, E.R., Seeliger, C., Vester, H., Kirschke, J.S., van Griensven, M., 2017. miRNAs in bone tissue correlate to bone mineral density and circulating miRNAs are gender independent in osteoporotic patients. Sci. Rep. 7 (1), 15861.

Kim, K., Dean, D., Lu, A., Mikos, A.G., Fisher, J.P., 2011. Early osteogenic signal expression of rat bone marrow stromal cells is influenced by both hydroxyapatite nanoparticle content and initial cell seeding density in biodegradable nanocomposite scaffolds. Acta. Biomaterialia. 7 (3), 1249–1264.

Kreke, M., Huckle, W., Goldstein, A., 2005. Fluid flow stimulates expression of osteopontin and bone sialoprotein by bone marrow stromal cells in a temporally dependent manner. Bone. 36 (6), 1047–1055.

Leboy, P.S., Grasso-Knight, G., D'Angelo, M., Volk, S.W., Lian, J.B., Drissi, H., Stein, G. S., Adams, S.L., 2001. Smad-Runx Interactions During Chondrocyte Maturation. J. Bone. Joint. Surg. Am. 83, S1–15–S1–22.

Li, M., Zhang, C., Li, X., Lv, Z., Chen, Y., Zhao, J., 2019. Isoquercitrin promotes the osteogenic differentiation of osteoblasts and BMSCs via the RUNX2 or BMP pathway. Connect. Tissue. Res. 60 (2), 189–199. https://doi.org/10.1080/03008207.2018.1483358.

Li, T., Li, H., Wang, Y., Li, T., Fan, J., Xiao, K.e., Zhao, R.C., Weng, X., 2016. microRNA-23a inhibits osteogenic differentiation of human bone marrow-derived mesenchymal stem cells by targeting LRP5. Int. J. Biochem. Cell. Biol. 72, 55–62.

Li, J., Tong, G., Huang, C., Luo, Y., Wang, S., Zhang, Y., Cheng, B., Zhang, Z., Wu, X., Liu, Q., Li, M., Li, L., Ni, B., 2020. Hoxc10 promotes cell migration, invasion, and tumor growth in gastric carcinoma cells through upregulating proinflammatory cytokines. J. Cell Physiol. 235 (1), 3579–3591.

Liao, W., Ning, Y., Xu, H.J., Zou, W., Hu, J., Liu, X., Yang, Y., Li, Z., 2019. BMSC-derived exosomes carrying microRNA-122-5p promote proliferation of osteoblasts in osteonecrosis of the femoral head. Clin. Sci. (Lond) 133 (18), 1955–1975.

Pan, W., Quarles, L.D., Song, L.-H., Yu, Y.-H., Jiao, C., Tang, H.-B., Jiang, C.-H., Deng, H.-W., Li, Y.-J., Zhou, H.-H., Xiao, Z.-S., 2005. Genistein stimulates the osteoblastic differentiation via NO/cGMP in bone marrow culture. J. Cell. Biochem. 94 (2), 307–316.

Ramírez-Salazar, E.G., Carrillo-Patiño, S., Hidalgo-Bravo, A., Rivera-Paredez, B., Quiterio, M., Ramírez-Palacios, P., Patiño, N., Valdés-Flores, M., Salmerón, J., Velázquez-Cruz, R., 2018. Serum miRNAs miR-140-3p and miR-23b-3p as potential biomarkers for osteoporosis and osteoporotic fracture in postmenopausal Mexican-Mestizo women. Gene. 679, 19–27.

Robinson, J.A., Chatterjee-Kishore, M., Yaworsky, P.J., Cullen, D.M., Zhao, W., Li, C., Kharode, Y., Sauter, L., Babij, P., Brown, E.L., Hill, A.A., Akhter, M.P., Johnson, M.L., Recker, R.R., Komm, B.S., Bex, F.J., 2016. Wnt/β-Catenin Signaling Is a Normal Physiological Response to Mechanical Loading in Bone. J. Biol. Chem. 281 (42), 31720–31728.

Shi, D., Sun, Y., Yin, J., Fan, X., Duan, H., Liu, N., He, W., 2014. Cajan leaf combined with bone marrow-derived mesenchymal stem cells for the treatment of osteonecrosis of the femoral head. Exp. Ther. Med. 7 (6), 1471–1475.

Shuai, B., Yang, Y.P., Lin, S., Wu, M., 2014. Effect of Qing'e Pill plus Salvia on Non-Traumatic Osteonecrosis of the Femoral Head of Idiopathic Type in Earlier Stage: A Case Report of a Twelve-Month of Period. Chin. Med. 5 (2), 113–117.

Wang, T., Teng, S., Zhang, Y., Wang, F., Ding, H., Guo, L., 2017. Role of mesenchymal stem cells on differentiation in steroid-induced avascular necrosis of the femoral head. Exp. Ther. Med. 13 (2), 669–675. https://doi.org/10.3892/etm.2016.3991.

Wang, X., Qian, W., Wu, Z., Bian, Y., Weng, X., 2014. Preliminary screening of differentially expressed circulating microRNAs in patients with steroidinduced osteonecrosis of the femoral head. Mol. Med. Rep. 10 (6), 3118–3124.

Wang, Y., Wang, R., Zhang, F., 2018. Icariin promotes the proliferation and differentiation of osteoblasts from the rat mandible by the Wnt/betacatenin signalling pathway. Mol. Med. Rep. 18 (3), 3445–3450.

Wang, L, Zhang, L., Chen, Z.B., Wu, J.Y., Zhang, X., Xu, Y., 2009. Icariin enhances neuronal survival after oxygen and glucose deprivation by increasing SIRT1. Eur. J. Pharmacol. 609 (1–3), 40–44.

Wu, X., Zhang, Y., Guo, X., Xu, H., Xu, Z., Duan, D., Wang, K., 2015. Identification of differentially expressed microRNAs involved in non-traumatic osteonecrosis through microRNA expression profiling. Gene. 565 (1), 22–29.

Xu, Y., Jiang, Y., Jia, B., Wang, Y., Li, T., 2021. Icariin stimulates osteogenesis and suppresses adipogenesis of human bone mesenchymal stem cells via miR-23a-mediated activation of the Wnt/β-catenin signaling pathway. Phytomedicine. 85, 153485. https://doi.org/10.1016/j.phymed.2021.153485.

Yang, H., Wu, L., Deng, H., Chen, Y., Zhou, H., Liu, M., Wang, S., Zheng, L., Zhu, L., Lv, X., 2020. Anti-inflammatory protein TSG-6 secreted by bone marrow mesenchymal stem cells attenuates neuropathic pain by inhibiting the TLR2/MyD88/NF-kappaB signaling pathway in spinal microglia. J. Neuroinflammation. 17 (1), 154.

Yin, J., Luo, Y., Deng, H., Qin, S., Tang, W., Zeng, L., Zhou, B., 2014. Hugan Qingzhi medication ameliorates hepatic steatosis by activating AMPK and PPARα pathways in L02 cells and HepG2 cells. J. Ethnopharmacol. 154 (1), 229–239.

Yu, H., Yue, Ju'an, Wang, W., Liu, P., Zuo, W., Guo, W., Zhang, Q., 2019. Icariin promotes angiogenesis in glucocorticoid-induced osteonecrosis of femoral heads: In vitro and in vivo studies. J. Cell. Mol. Med. 23 (11), 7320–7330.

Yuan, H.F., Von Roemeling, C., Gao, H.D., Zhang, J., Guo, C.A., Yan, Z.Q., 2015. Analysis of altered microRNA expression profile in the reparative interface of the femoral head with osteonecrosis. Exp. Mol. Pathol. 98 (2), 158–163.

Zhao, J., Ohba, S., Shinkai, M., Chung, U.I., Nagamune, T., 2008. Icariin induces osteogenic differentiation in vitro in a BMP- and Runx2-dependent manner. Biochem. Biophys. Res. Commun. 369 (2), 444–448. https://doi.org/10.1016/j.bbrc.2008.02.054.

Zhao, J., Ohba, S., Komiyama, Y., Shinkai, M., Chung, U.-i., Nagamune, T., 2010. Icariin: a potential osteoinductive compound for bone tissue engineering. Tissue. Eng. Part. A 16 (1), 233–243.

Zhang, X.Y., Chen, Y.P., Zhang, C., Zhang, X., Xia, T., Han, J., Yang, N., Song, S., Xu, C., 2020. Icariin accelerate fracture healing via activation of WNT1/β-catenin osteogenic signaling pathway. Cur. Pharma. Biotech. 21. https://doi.org/10.2174/1389201021666200611121539.

Zhang, Y., Li, Q., Zhang, Y., Wang, Z., 2010. Morphology and immunohistochemistry of traumatic and non-traumatic necrosis of the femoral head. Zhongguo Xiu Fu Chong Jian Wai Ke Za Zhi. 24 (1), 17–22.

Zhang, Y., Shen, F., Mao, Z., Wang, N., Wang, Y., Huang, X., Hu, Y., Shou, D., Wen, C., 2017a. Icariin Enhances Bone Repair in Rabbits with Bone Infection during Post-infection Treatment and Prevents Inhibition of Osteoblasts by Vancomycin. Front. Pharmacol. 8, 784–796.

Zhang, G., Liu, X., Li, Y., Wang, Y., Liang, H., Li, K., Li, L., Chen, C., Sun, W., Ren, S., Zhu, P., Zhang, L., 2017b. EphB3-targeted regulation of miR-149 in the migration and invasion of human colonic carcinoma HCT116 and SW620 cells. Can Sci. 108 (3), 408–418.

Zhang, J., Tang, C., Liao, W., Zhu, M., Liu, M., Sun, N., 2019. The antiapoptotic and antioxidative stress effects of Zhisanzhen in the Alzheimer's disease model rat. Neuroreport. 30 (9), 628–636.